May 1999

ELSEVIER

Materials Letters 39 (1999) 232–239

MATERIALS LETTERS

www.elsevier.com/locate/matlet

Optical properties of thin-film ternary $Ge_{10}As_{15}Se_{75}$ chalcogenide glasses

J.M. González-Leal [a], A. Ledesma [a], A.M. Bernal-Oliva [a], R. Prieto-Alcón [a], E. Márquez [a,*], J.A. Angel [a], J. Cárabe [b]

[a] *Departamento de Física de la Materia Condensada, Facultad de Ciencias, Universidad de Cádiz, Apdo. 40, 11510-Puerto Real, Cádiz, Spain*

[b] *CIEMAT, Avda. Complutense, 22, ed. 42, 28040 Madrid, Spain*

Received 5 November 1998; accepted 7 December 1998

Abstract

The optical properties of ternary chalcogenide amorphous thin films of chemical composition $Ge_{10}As_{15}Se_{75}$, deposited by vacuum thermal evaporation, have been determined and analysed. Normal-incidence optical transmission spectra have been measured in the range from 400 to 2500 nm. From these transmission spectra, the optical constants and average thickness of this particular amorphous ternary material were accurately calculated using an optical-characterisation method based on creating the upper and lower envelope curves of the spectrum, which also allows to obtain a parameter indicating the degree of film-thickness uniformity. The dispersion of the refractive index is discussed in terms of the single-oscillator Wemple–DiDomenico model. The optical-absorption edge is described using the non-direct transition model proposed by Tauc and the optical band gap is calculated from the absorption coefficient values by Tauc's extrapolation procedure. A comparison between these optical properties and those corresponding to the $As_{30}Se_{70}$ and $Ge_{25}Se_{75}$ binary thin films (previously reported) is also presented.

PACS: 73.61Jc; 78.20Ci

Keywords: Chalcogenide glasses; Thin films; Optical characterisation

1. Introduction

Chalcogenide glasses are very well known semiconductor materials owing to their high transmittance in the IR spectral region [1] and to the variety of phenomena they show when exposed to light or other radiation [2–6]. Different kinds of photoinduced structural or physico-chemical changes in amorphous chalcogenides have been observed, such as: photocrystallisation, photopolymerisation, photodecomposition, photoinduced morphological changes, photovaporisation, photodissolution of certain metals and photovitrification [2,3] and light-induced changes in local atomic configuration [4–6]. In general, these phenomena are associated with significant changes in the optical constants [7,8] and absorption-edge shifts (i.e., photodarkening or photobleaching), allowing the use of these materials in the fabrication of a great number of optical devices

* Corresponding author. Tel.: +34-956-830966; Fax: +34-956-834924; E-mail: juanmaria.gonzalez@uca.es

00167-577X/99/$ - see front matter
PII: S0167-577X(99)00012-9

[9–11]. Therefore, the accurate determination of the optical constants of these materials is important, not only in order to know the basic mechanisms underlying these phenomena, but also to exploit and develop their interesting technological applications.

The optical characterisation of thin films often requires the use of highly refined computer numerical techniques applied to both optical transmission and reflection spectra [12–15]. In contrast, a relatively simple and straightforward method for determining the optical constants, using only the transmission spectra, has been proposed by Swanepoel [16], which is also particularly useful because it accounts for a possible lack of film-thickness uniformity. This method is based on the upper and lower envelopes of normal-incidence optical transmission spectra, and takes into account the spectrum compression (i.e., increase of minima and decrease of maxima of interference) caused by film-thickness variations across the light spot defined by the spectrophotometer beam. Since the samples being the object of the present study were thin films with relatively non-uniform thicknesses, said method was successfully applied. The samples were layers of a ternary amorphous material having a chemical composition $Ge_{10}As_{15}Se_{75}$, deposited onto glass substrates by vacuum thermal evaporation. Accurate values for the optical constants and film thickness were obtained. The present study is of particular interest given the scarcity of literature on the optical properties of ternary-chalcogenide-glass thin films.

2. Experimental procedure

The samples studied in the present work were $Ge_{10}As_{15}Se_{75}$ amorphous thin films deposited by vacuum thermal evaporation onto glass transparent substrates (microscope slides BDH, model Superpremium) from an ingot of the same amorphous material, made by using the well-known melt-quenching technique. The thermal evaporation process was performed by means of a coating system (Edwards, model E306A), with a pressure of about 10^{-6} Torr, using a suitable quartz crucible. The growth rate was continuously measured with a quartz oscillator (Edwards, model FTM-5) and was controlled during the whole process to be kept at ≈ 0.5 nm s^{-1}. Such a low growth rate yields films having a composition very similar to that of the original bulk sample [17]. The possible differences between the compositions of the evaporation source material and the film deposited onto the substrate were determined by Energy-Dispersive X-ray Analysis (EDAX), by making use of a scanning electron microscope (Jeol, model JSM-820). The results show that the composition of the thin films grown is equal to that of the bulk source material within ± 2 at.%. The thickness of the layers studied ranges from 800 to 1200 nm. The normal-incidence transmission spectra were measured in the range 400–2500 nm by means of a double-beam, ratio-recording, UV/Vis/NIR computer-controlled spectrophotometer (Perkin Elmer, model Lambda-19). All optical measurements reported were performed at room temperature.

3. Theoretical basis

One of the main difficulties faced in the present work was the accurate optical characterisation of thin films whose thicknesses were only approximately uniform across the samples. In other words, the use of an appropriate method was essential in order to make sure that the results would make sense. The model behind such a method therefore assumes that the sample is a thin film of non-uniform thickness deposited on a transparent substrate having a refractive index s. The system is surrounded by air, whose refractive index is $n_0 = 1$. The film has a complex refractive index $n_c = n - ik$, where n is the refractive index and k the extinction coefficient, which is related to the absorption coefficient, α, through the expression: $k = \alpha\lambda/4\pi$. If a linear variation is assumed along the spot defined by the spectrophotometer beam (1×10 mm^2 approximately), the thickness d can be expressed as: $d = \bar{d} + \eta\Delta d$ with $-1 \leq \eta \leq 1$, where the parameter Δd is a measure of the thickness deviation at the limits of the spot with respect to the average film thickness, $\bar{d}$ (see Fig. 1). Under these considerations, the spectral transmittance $T(\lambda)$, for any wavelength λ in the transparent region, is given by Eq. (10) from Ref. [16], and the upper, $T_M(\lambda)$, and lower, $T_m(\lambda)$, en-

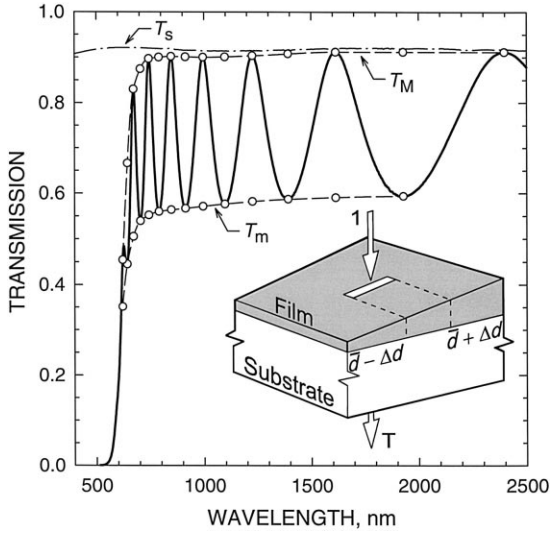

Fig. 1. Optical-transmission spectrum at normal incidence of a film of non-uniform thickness, being representative of the samples studied (ternary vitreous material having a composition Ge_{10}-$As_{15}Se_{75}$). Curves T_M and T_m are the upper and lower envelopes, respectively and T_s is the transmission spectrum of the substrate alone. The tangent points between the envelopes and the transmission spectrum are indicated. A scheme of the optical system under study is also shown.

velopes of the optical transmission spectrum, have the following expressions:

$$T_{M,m}(\lambda) = \frac{\lambda}{2\pi n\Delta d}\frac{a}{(1-b^2)^{1/2}}\tan^{-1}\times\left[\frac{1\pm b}{(1-b^2)^{1/2}}\tan\left(\frac{2\pi n\Delta d}{\lambda}\right)\right], \quad (1)$$

where $a = A/(B+D)$, $b = C/(B+D)$, $A = 16n^2 s$, $B = (n+1)^3\ (n+s^2)$, $C = 2(n^2-1)(n-s^2)$ and $D = (n-1)^3\ (n-s^2)$. The positive sign in '$\pm$' corresponds to $T_M(\lambda)$ and the negative one to $T_m(\lambda)$. The equations expressed in Eq. (1) are valid as long as the condition $0 < \Delta d < \lambda/4n$ holds. The values of the substrate refractive index for the whole spectral range are obtained from the stand-alone-substrate transmission spectrum, T_s, by using the following expression [16,18]:

$$s = \frac{1}{T_s} + \left(\frac{1}{T_s^2} - 1\right)^{1/2}. \quad (2)$$

Therefore, the expressions covered by Eq. (1) are two independent transcendental equations having only two unknown parameters, n and Δd. This equation set can be solved, in general, for all the wavelengths in the transparent region, by using some method for the solution of transcendental equations, such as the Newton–Raphson iterative method. Solving in particular only for those wavelengths for which the envelopes and the spectrum are mutually tangent, preliminary refractive-index values, n_1, and a set of values for Δd, are calculated. The low statistical scatter observed in the latter, allows to take their average as an excellent approximation of the lack of thickness uniformity of the film.

It should be stressed that, owing to absorption, the well known basic interference equation:

$$2n\bar{d} = m\lambda, \quad (3)$$

will not be valid in the interference maxima and minima, i.e., in those points for which $dT(\lambda)/d\lambda = 0$, but in the above mentioned tangent points [16]. This equation can be used for drawing an initial approximation of the average film thickness by means of the following expression, derived from Eq. (3):

$$d_1 = \frac{\lambda'\lambda''}{4(n_1''\lambda' - n_1'\lambda'')}, \quad (4)$$

where n_1' and n_1'' are the refractive indexes for two adjacent tangent points having wavelengths λ' and λ'', respectively. In addition, applying again Eq. (3) and using d_1 mean value, $\bar{d}_1$, and the previously obtained refractive indexes, n_1, the corresponding interference order numbers, m_0, can be estimated. The exact order numbers, m, being integers for the upper tangent points and half-integers for the lower tangent points, are obtained by rounding the m_0 values. Then, from n_1 and m, Eq. (3) can be solved in order to determine the average film thickness, d_2, more accurately. The mean of these values, $\bar{d}_2$, will be eventually taken as the average film thickness. Finally, replacing $\bar{d}_2$ and m again in Eq. (3), the ultimate refractive-index values, n_2, for the tangent points are derived. A subsequent fit of these refractive-index values to a specific dispersion model allows their extrapolation to the interference-free spectral region.

In the case of a uniform thin film, the absorbance, x, can be extracted from the upper envelope by means of the expression [16,18]:

$$x = \frac{E_M - \left[E_M^2 - (n^2-1)^3(n^2-s^4)\right]^{1/2}}{(n-1)^3(n-s^2)}, \qquad (5)$$

where

$$E_M = \frac{8n^2 s}{T_M} + (n^2-1)(n^2-s^2).$$

These formulae also hold for films of non-uniform thickness in the interference-free spectral region, where upper and lower envelopes converge to a single curve, $T_M(\lambda) = T_m(\lambda) = T(\lambda)$ [16]. Nonetheless, once interference influences transmission, i.e., when $T_M(\lambda) \neq T_m(\lambda)$, the spectrum compression affects the values of T_M and, thus, the absorbance derived from Eq. (5). In such a case, the material tends to seem to be more absorbent than it actually is, originating an absorption-edge tail [16]. Finally, once the absorbance, x, and the average film thickness, $\bar{d}_2$, are known, the equation $x = \exp(-\alpha \bar{d}_2)$ can be solved in order to obtain the absorption coefficient. The extinction coefficient is furthermore determined from the relation $k = \alpha\lambda/4\pi$.

The absorption coefficient of amorphous semiconductors in the strong-absorption region ($\alpha \gtrsim 10^4$ cm^{-1}), assuming parabolic valence- and conduction-band edges, is given according to the model proposed by Tauc [19], by the following expression:

$$\alpha(\hbar\omega) = \frac{B\left(\hbar\omega - E_g^{opt}\right)^2}{\hbar\omega}, \qquad (6)$$

where $\hbar\omega$, E_g^{opt} and B, represent photon energy, optical gap and an energy-independent constant, respectively. Finally, the optical gap is obtained from the intersection of the plot $(\alpha\hbar\omega)^{1/2}$ vs. $\hbar\omega$ with the abscissa axis.

4. Results and discussion

Fig. 1 shows the normal-incidence optical transmission spectrum of a sample representative of those under study, having a chemical composition $Ge_{10}As_{15}Se_{75}$, together with the spectrum corresponding to the substrate onto which it has been deposited. In the said figure, the envelopes of the transmission spectrum, T_M and T_m, can also be observed. Such envelopes have been computer generated by using software specifically designed for this purpose [20]. The points for those wavelengths for which the envelopes and the transmission spectrum are tangent are also drawn. Columns n_1 and Δd of Table 1 contain the refractive indexes and thick-

Table 1
Values of λ, s, T_M and T_m corresponding to the optical transmission spectrum of Fig. 1

λ (nm)	s	T_M	T_m	n_1	Δd (nm)	d_1 (nm)	m_0	m	d_2 (nm)	n_2
1929	1.513	0.912	0.594	2.573	27	–	2.5	2.5	937	2.576
1614	1.516	0.912	0.591	2.584	21	936	3.0	3.0	937	2.587
1392	1.531	0.907	0.587	2.609	19	915	3.51	3.5	934	2.603
1225	1.539	0.903	0.582	2.636	18	899	4.03	4.0	929	2.618
1097	1.543	0.901	0.577	2.661	17	915	4.54	4.5	928	2.637
995	1.534	0.900	0.571	2.678	17	939	5.04	5.0	929	2.658
913	1.533	0.901	0.567	2.693	15	968	5.52	5.5	932	2.682
847	1.513	0.902	0.564	2.696	16	1072	5.96	6.0	942	2.715
790	1.518	0.900	0.560	2.715	15	986	6.43	6.5	946	2.743
743	1.517	0.897	0.552	2.748	14	954	6.92	7.0	946	2.778
704	1.510	0.875	0.539	2.830	19	780	7.52	7.5	933	2.821
672	1.510	0.830	0.506	3.039	22	–	8.46	8.0	–	2.872
643	1.510	0.666	0.445	3.709	29	–	10.8	8.5	–	2.920
621	1.509	0.454	0.351	5.304	25	–	16.0	9.0	–	2.986

$\bar{d}_1 = 936 \pm 74$ nm (7.9%); $\bar{d}_2 = 936 \pm 7$ nm (0.7%)

Calculation of the thickness and the refractive index based on the present optical method.

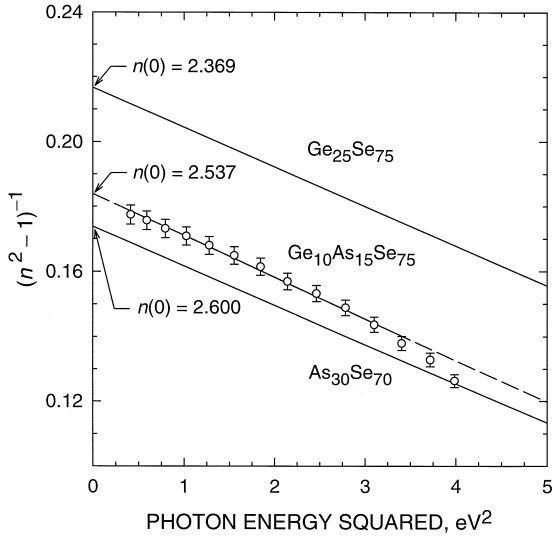

Fig. 2. Linearisation of the Wemple–DiDomenico model for the calculation of the dispersion parameters corresponding to the ternary compound studied, as well as to those binary compounds found in the literature, having the same or a similar selenium content, $Ge_{25}Se_{75}$ and $As_{30}Se_{70}$. The values of the static refractive index, $n(0)$, show a marked decrease with germanium content.

ness variations calculated for such points from equation set (1), solved by using the Newton–Raphson iteration method. The low statistical scatter of these results is noticeable and highlights the validity of the method. The value of Δd obtained for the representative film under study is 20 ± 5 nm. The accuracy of the refractive index, n_1, can be improved by means of Eq. (3), using the above described method, shown in Table 1, where the final refractive index is listed in column n_2. The final average film thickness of the representative sample is 936 ± 7 nm (0.7%).

On the other hand, the refractive-index values obtained can be fit to the Wemple–DiDomenico dispersion model, based on the single oscillator [21,22]:

$$n^2(\hbar\omega) = 1 + \frac{E_d E_0}{E_0^2 - (\hbar\omega)^2}, \qquad (7)$$

where E_0 is the oscillator energy and E_d is the dispersion energy. Representing $(n^2-1)^{-1}$ vs. $(\hbar\omega)^2$ and performing a linear fit, shown in Fig. 2, E_d y E_0 can be directly determined from the slope, $(E_0 E_d)^{-1}$, and the intercept, E_0/E_d, on vertical axis. The equation of the fit for the representative $Ge_{10}As_{15}Se_{75}$ thin film sample is $(n^2-1)^{-1} = 0.184–0.013\ (\hbar\omega)^2$, with a correlation coefficient better than 0.996. The values obtained for the dispersion parameters, E_0 y E_d, and for the static refractive index, $n(0)$ (i.e., extrapolated to $\hbar\omega \to 0$), for the $Ge_{10}As_{15}Se_{75}$ ternary thin film, as well as the values of these parameters found in the literature, for those binary compounds having a Se content equal or similar to that of the ternary compound under study, $Ge_{25}Se_{75}$ [23] and $As_{30}Se_{70}$ [24], are summarised in Table 2. The agreement of the different parameters that are reported in this work with those of the binary compounds is noticeable. In particular, a higher dispersion parameter, E_0, is observed, whereas E_d and $n(0)$, decrease with the germanium content. The refractive-index dispersion from the Wemple–DiDomenico model is shown in Fig. 3, together with the refractive indexes derived using the present characterization method.

Parameter E_0 is an 'average' energy gap and, with a very good approximation, can be related to the optical gap, E_g^{opt}, through the relation $E_0 \approx 2 \times E_g^{opt}$, obtained by Tanaka [25] when studying vitreous films having a composition As_xS_{100-x}, and which holds also for other vitreous chalcogenide alloys [23,24,26]. Furthermore, the dispersion parameter E_0,

Table 2
Values of the single-oscillator energy (E_0), dispersion energy (E_d), refractive index at $\hbar\omega \to 0$ ($n(0)$), Tauc optical gap (E_g^{opt}), gap ratio (E_0/E_g^{opt}), Tauc slope ($B^{1/2}$), an alternative option for the optical gap (E_{04}) and the slope parameter of the Urbach region (E_e)

Composition	E_0 (eV)	E_d (eV)	$n(0)$	E_g^{opt} (eV)	E_0/E_g^{opt}	$B^{1/2}$ ($cm^{-1/2}\ eV^{-1/2}$)	E_{04} (eV)	E_e (meV)
$As_{30}Se_{70}$ [24]	3.79	21.81	2.600	1.82	2.08	1321	–	–
$Ge_{10}As_{15}Se_{75}$	3.78 ± 0.05	20.57 ± 0.3	2.537 ± 0.004	1.89 ± 0.01	2.00	928 ± 2	2.03 ± 0.01	82 ± 1
$Ge_{25}Se_{75}$ [23]	4.21	19.43	2.369	2.03	2.04	806	–	80

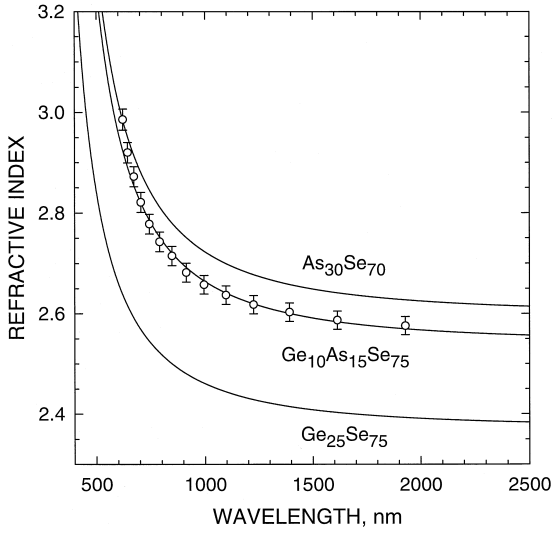

Fig. 3. Refractive index versus wavelength. The curves have been generated from the Wemple–DiDomenico dispersion model.

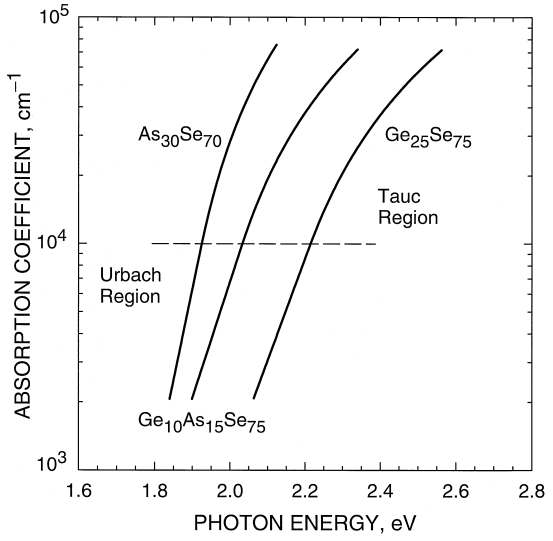

Fig. 4. Semi-logarithmic plot of the absorption coefficient as a function of photon energy for the sample representative of the ternary compound $Ge_{10}As_{15}Se_{75}$, and for those binary compounds cited in the present work. There is a distinct absorption-edge shift towards higher photon energies for increasing germanium contents.

can be identified with the mean transition energy from the valence band of lone-pair p-states, characteristic of these vitreous materials, to conduction-band states. In addition, E_d also obeys a simple empirical relation [21,22], $E_d = \beta N_c Z_a N_e$, where β is a constant which, for covalent crystalline and amorphous materials, has a value of ≈ 0.4 eV, N_c is the coordination number of the cation nearest neighbour of the anion, Z_a is the formal chemical valence of the anion and N_e is the effective number of valence electrons per anion. In particular, from the value of E_d obtained, and assuming $N_e = (10 \times 4 + 15 \times 5 + 75 \times 6)/75 = 113/15$ and $Z_a = 2$, the corresponding N_c is ≈ 3.41. This value is in excellent agreement with the theoretical coordination number expected, i.e., re-writing the composition under study in the form $(Ge_{0.4}As_{0.6})_{25}Se_{75}$, $Ge_{0.4}As_{0.6}$ could be considered as a hypothetical cation whose coordination number would be: $N_c^{theor} = 0.4 \times 4 + 0.6 \times 3 = 3.40$. This result denotes the accuracy of the refractive indexes and, thus, that of the film thickness, both derived from the optical-characterisation method described.

The optical-absorption spectrum calculated from the absorbance, x, as derived from Eq. (5), is plotted in Fig. 4. Furthermore, Fig. 5 shows $(\alpha\hbar\omega)^{1/2}$ vs. $\hbar\omega$, for the calculation of the optical gap, E_g^{opt}. The values of E_g^{opt} and of the slope $B^{1/2}$, drawn from the Tauc plot, appear in Table 2, in addition to an alternative optical gap, E_{04}, defined as the energy for

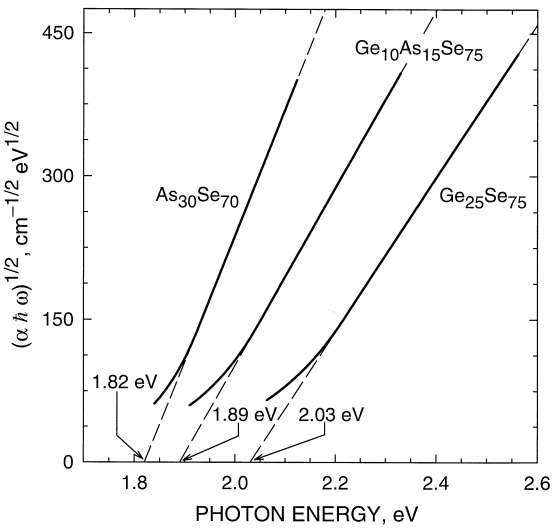

Fig. 5. Tauc plot for calculating the optical gap of the ternary compound $Ge_{10}As_{15}Se_{75}$, and of the binary compounds $Ge_{25}Se_{75}$ and $As_{30}Se_{70}$.

which $\alpha = 10^4$ cm^{-1}, for the ternary compound under study, as well as for the above mentioned binary compounds [23,24]. Similarly to what occurred with the dispersion parameters, the values of the parameters of the model in the strong-absorption region are highly consistent when a comparison is made between the results for the different chemical compositions. In this case, E_g^{opt} rises with the germanium content. This effect can be explained in terms of the higher bonding energy of Ge–Se (473 kJ mol^{-1}), with respect to As–Se (96 kJ mol^{-1}). Moreover, as can be seen in Table 2, the values of E_0 clearly satisfy the above-mentioned relation, $E_0 \approx 2 \times E_g^{opt}$. Finally, the difference between the optical-gap value obtained for amorphous films having a glassy composition $Ge_{10}As_{15}Se_{75}$, and that reported for thin films of the same chemical composition by El-Samanoudy et al. [27] ($E_g^{opt} = 1.81$ eV), $\approx 4\%$, may be explained considering that in Ref. [27], the calculation of the absorption coefficients is carried out only approximately by use of the well-known Lambert–Beer law: $I = I_0 \exp(-\alpha d)$, where I and I_0 are the intensities of the transmitted and incident beams, respectively. However, this expression does not take into account, obviously, the multiple reflections at the different interfaces of the optical system analysed, which can lead to significant errors in the values obtained for α.

Lastly, for absorption-coefficient values such that 10 cm$^{-1} \lesssim \alpha \lesssim 10^4$ cm^{-1}, the absorption is due to electronic transitions between valence-band-tail and conduction-band states and depends exponentially on photon energy according to the Urbach relation [19]:

$$\alpha = \alpha_0 \exp\left(\frac{\hbar\omega}{E_e}\right), \tag{8}$$

where E_e is the so-called Urbach slope, whose value is typically between 50 and 90 meV. The value of E_e obtained for the specimen representative of the composition $Ge_{10}Se_{15}As_{75}$ is 82 meV.

Finally, it should be stressed that the specimens were subject to thermal-annealing processes at temperatures close to that of the glass transition ($T_g \approx$ 143°C), and illumination with light of photon energy near the optical gap, without detecting any relevant changes in their optical properties. This behaviour is probably due to the high selenium content [28] and to the relaxation of the samples since their fabrication (approximately 6 months earlier) [29,30].

5. Conclusions

The optical properties of ternary $Ge_{10}As_{15}Se_{75}$ chalcogenide-glass thin films (thickness between 800 and 1200 nm) have been thoroughly investigated and compared to those of related binary compounds, such as $Ge_{25}Se_{75}$ and $As_{30}Se_{70}$. The optical-characterisation method applied has allowed to overcome the problem of non-uniform film thickness, which causes a decrease in interference maxima and an increase in minima for decreasing wavelengths, and which would yield significant errors if not taken into account. The procedure has given refractive indexes and average thicknesses within $\approx 1\%$ accuracy. Finally, it should be noted the excellent consistency that has been found between the results obtained in the present work and those previously reported by other authors for related binary compounds: parameters E_0 and E_g^{opt} increase, whereas E_d and $n(0)$, decrease with germanium content. This investigation is considered of special interest given the scarcity of optical data on these materials available in the literature.

Acknowledgements

The authors would like to acknowledge the CICYT of Spain for financial support through project MAT98-0791.

References

[1] J.A. Savage, Infrared Optical Materials and Their Antireflection Coatings, Adam Hilger, Bristol, 1985.
[2] E. Márquez, R. Jiménez-Garay, A. Zakery, P.J.S. Ewen, A.E. Owen, Philos. Mag. B 63 (1991) 1169.
[3] E. Márquez, C. Corrales, J.B. Ramírez-Malo, J. Reyes, J. Fernández-Peña, P. Villares, R. Jiménez-Garay, Mater. Lett. 20 (1994) 183.
[4] A.E. Owen, A.P. Firth, P.J.S. Ewen, Philos. Mag. B 52 (1985) 347.
[5] S.R. Elliott, Physics of Amorphous Materials, Longman, New York, 1990.

[6] P.J.S. Ewen, A.E. Owen, High-performance Glasses, Blackie, London, 1992.
[7] E. Márquez, J.B. Ramírez-Malo, J. Fernández-Peña, P. Villares, R. Jiménez-Garay, P.J.S. Ewen, A.E. Owen, J. Non-Cryst. Solids 164–166 (1993) 1223.
[8] E. Márquez, J.B. Ramírez-Malo, J. Fernández-Peña, R. Jiménez-Garay, P.J.S. Ewen, A.E. Owen, Opt. Mater. 2 (1993) 143.
[9] J. Tauc, Amorphous and Liquid Semiconductors, Plenum, New York, 1974.
[10] Z. Cimpl, F. Kosek, Phys. Stat. Sol. (a) 93 (1986) K55.
[11] D.A. Minkov, E. Vateva, E. Skordeva, D. Arsova, M. Nikiforova, J. Non-Cryst. Solids 90 (1987) 481.
[12] J. Szcyrbrowski, A. Czapla, Thin Solid Films 46 (1977) 127.
[13] L. Vriens, W. Rippens, Appl. Opt. 22 (1983) 4105.
[14] D.P. Arndt, R.M.A. Azzam, J.M. Bennett, J.P. Borgogno, C.K. Carniglia, W.E. Case, J.A. Dobrowolski, U.J. Gibson, T. Tuttle Hart, F.C. Ho, V.A. Hodgkin, W.P. Klapp, H.A. Macleod, E. Pelletier, M.K. Purvis, D.M. Quinn, D.H. Strome, R. Swenson, P.A. Temple, T.F. Thonn, Appl. Opt. 23 (1984) 3571.
[15] D.A. Minkov, J. Mod. Optic 37 (1990) 1977.
[16] R. Swanepoel, J. Phys. E: Sci. Instrum. 17 (1984) 896.
[17] K. White, B. Kumar, A.K. Rai, Thin Solid Films 161 (1988) 139–147.
[18] R. Swanepoel, J. Phys. E: Sci. Instrum. 16 (1983) 1214.
[19] J. Tauc, J. Non-Cryst. Solids 8–10 (1972) 569.
[20] M. McClain, A. Feldman, D. Kahaner, X. Ying, Comput. Phys. 5 (1991) 45.
[21] S.H. Wemple, W. DiDomemico, Phys. Rev. B 3 (1971) 1338.
[22] S.H. Wemple, Phys. Rev. B 8 (1973) 3767.
[23] J. Reyes, E. Márquez, J.B. Ramírez-Malo, C. Corrales, J. Fernández-Peña, P. Villares, R. Jiménez-Garay, J. Mater. Sci. 30 (1995) 4133.
[24] C. Corrales, PhD Thesis, University of Cádiz, 1994.
[25] Ke. Tanaka, Thin Solid Films 66 (1980) 271.
[26] T.I. Kosa, T. Wagner, P.J.S. Ewen, A.E. Owen, Philos. Mag. B 71 (1995) 311.
[27] M.M. El-Samanoudy, M. Fadel, J. Mater. Sci. 27 (1992) 646.
[28] G. Pfeiffer, M.A. Paesler, S.C. Agarwal, J. Non-Cryst. Solids 130 (1991) 111.
[29] J. Teteris, O. Nordman, J. Opt. Soc. Am. B 14 (1997) 2498.
[30] O. Nordman, N. Nordman, J. Teteris, Opt. Commun. 146 (1998) 69.